



HAL
open science

High-frequency non-tidal ocean loading effects on surface gravity measurements

Jean-Paul Boy, Florent Lyard

► **To cite this version:**

Jean-Paul Boy, Florent Lyard. High-frequency non-tidal ocean loading effects on surface gravity measurements. *Geophysical Journal International*, 2008, 175 (1), pp.35-45. 10.1111/j.1365-246X.2008.03895.x . hal-00409302

HAL Id: hal-00409302

<https://hal.science/hal-00409302>

Submitted on 18 Jun 2021

HAL is a multi-disciplinary open access archive for the deposit and dissemination of scientific research documents, whether they are published or not. The documents may come from teaching and research institutions in France or abroad, or from public or private research centers.

L'archive ouverte pluridisciplinaire **HAL**, est destinée au dépôt et à la diffusion de documents scientifiques de niveau recherche, publiés ou non, émanant des établissements d'enseignement et de recherche français ou étrangers, des laboratoires publics ou privés.

High-frequency non-tidal ocean loading effects on surface gravity measurements

Jean Paul Boy¹ and Florent Lyard²

¹*EOST-IPGS (UMR 7516 CNRS-ULP), 5 rue Rene Descartes, 67084 Strasbourg, France. E-mail: jpboy@eost.u-strasbg.fr*

²*LEGOS (UMR 5566), 14 Avenue Edouard Belin, 31400 Toulouse, France*

Accepted 2008 June 23. Received 2008 June 23; in original form 2008 March 12

SUMMARY

We model atmospheric and non-tidal oceanic loading effects on surface gravity variations, using global surface pressure field provided by the European Centre for Medium-range Weather Forecasts (ECMWF), and sea surface height from the Toulouse Hydrodynamic Unstructured Grid Ocean model (HUGO-m) barotropic ocean model. We show the improvement in terms of reduction of variance of 15 different superconducting gravimeters of the worldwide Global Geodynamics Project (GGP) network, compared to the classical inverted barometer assumption.

We also study two storm surges over the Western European Shelf in 2000 and 2003. We compare the HUGO-m sea surface height variations to various tide gauges measurements as well as the induced loading effects to the computations of Fratepietro *et al.*, using the Proudman Storm Surge model, for the Membach (Belgium) station. The agreement between modelled ocean loading and gravity observations is largely improved when using a global atmospheric loading correction, compared to the classical local approach. The remaining discrepancies are mainly due to hydrological loading contributions.

Key words: Sea level change; Time variable gravity.

1 INTRODUCTION

Atmospheric loading is, besides solid Earth tides and ocean tidal loading, one of the major sources of surface gravity perturbations over a wide frequency domain (see, for example, Boy *et al.* 2002). With the help of global atmospheric data sets provided by meteorological centres and Green's function formalism (Farrell 1972), the atmospheric loading can easily be computed (Boy *et al.* 2002) and can reduce gravity residuals over a large frequency band (from typically a few days to 100 days). The main limitation of these computations is the assumption of a simple ocean response to pressure forcing: the 'non-inverted barometer' (NIB) or the 'inverted barometer' (IB) hypotheses (Wunsch & Stammer 1997). In a previous study (Boy *et al.* 2002), we have shown that the NIB assumption cannot be a valid model for estimating the ocean response to pressure forcing. We here show the improvement in reduction of gravity residuals, by adding to our global atmospheric loading computations, the effects due to the dynamic barotropic ocean response to air pressure and wind forcing.

Non-tidal oceanic loading effects on superconducting gravimeters have already been studied by, for example, Virtanen (2004) and Zerbini *et al.* (2004). However, they were looking at lower frequencies (typically seasonal timescales). For these periods, the oceanic circulation is mostly forced by heat and fresh water fluxes and winds, and the oceans cannot be considered as barotropic. The high-frequency barotropic oceanic loading effects on surface grav-

ity have been modelled by Fratepietro *et al.* (2006) for the station of Membach (Belgium) and for a 2 week period, corresponding to a storm surge occurring over the North Sea. However, they suggested to use non-tidal ocean models, forced by air pressure and winds, such as MOG2D (Carrère & Lyard 2003), for better non-tidal ocean loading corrections on gravity measurements.

In this paper, we are adding to our atmospheric loading estimates, using surface pressure field provided by the European Centre for Medium-Range Weather Forecasts (ECMWF), non-tidal ocean loading computed using the Toulouse Hydrodynamic Unstructured Grid Ocean model (HUGO-m) (MOG2D follow-on) barotropic ocean model forced by ECMWF pressure and wind fields (Carrère & Lyard 2003). This model is also currently used for the Gravity Recovery And Climate Experiment (GRACE) (Lemoine *et al.* 2007) and radar altimetry processing.

Other ocean models forced by air pressure and winds are also currently available, thanks to the GRACE project (Flechtner 2005): the so-called PPHA (Hirose *et al.* 2001) barotropic, and the Ocean Model for Circulation and Tides (OMCT) (Dobslaw & Thomas 2005) baroclinic ocean models. However their spatial resolution (1.125° for PPHA and 1.875° for OMCT) do not allow a precise estimation of oceanic mass variations over continental shelves, which have been shown to have a significant contribution to surface gravity changes (Fratepietro *et al.* 2006). On the other hand, the lack of the Arctic ocean in the PPHA model do not allow to model high frequency non-tidal ocean loading in Ny-Alesund (Svalbard), one

of the stations of the Global Geodynamic Project (GGP) network (Crossley *et al.* 1999).

As we are studying the high frequency surface gravity variations (periods smaller than typically a few months), we choose to model the atmospheric loading effects using only surface pressure data following Merriam (1992) and Boy *et al.* (2002), and not the complete 3-D structure of the atmosphere, as Neumeier *et al.* (2004) showed that the differences between the 2-D and 3-D approaches are larger at seasonal timescales (differences of about $1 \mu\text{Gal}$).

In Section 2, we present the computations of atmospheric and oceanic loading effects, from surface pressure field provided by ECMWF, and sea surface height variations from the HUGO-m barotropic ocean model. In Section 3, we show the reduction of gravity residuals using HUGO-m, compared to the classical NIB and IB approaches. Section 4 is devoted to the study of some storm surges occurring in the North Sea, with a comparison with Fratetiro *et al.* (2006). Discussion and concluding remarks are given in Section 5.

2 ATMOSPHERIC AND OCEANIC LOADING COMPUTATIONS

2.1 Comparison between the IB assumption and the barotropic model

We are using 6-hourly sea surface height outputs of the HUGO-m barotropic ocean model, forced by 6-hourly ECMWF surface pressure and winds, given on a regular 0.5° global grid, obtained by an interpolation of the native finite element grid (Carrère & Lyard 2003).

Fig. 1 shows the root mean square (rms) differences between the IB assumption and HUGO-m sea surface height, computed for the

2000–2006 period. The larger differences occur over shallow water regions, such as the European, the Patagonia shelves, and along the Arctic Sea coast; they can reach up to 25 cm. Due to the large pressure and wind forcing, the differences can be as large as 10 cm around Antarctica.

Fig. 1 also exhibits the lack of some small enclosed or semi-enclosed basins (shown in grey) in HUGO-m. As Virtanen (2004) showed, there is a strong correlation between Metsähovi (Finland) gravity residuals and tide gauge measurements in the Baltic Sea. The lack of the Baltic Sea in HUGO-m may lead us to a lower reduction of residuals variance for this station, compared to other European instruments.

2.2 Green's function formalism

Surface gravity variations are computed through a convolution of Green's functions (Farrell 1972) and surface pressure field provided by the ECMWF or barotropic sea surface height from the HUGO-m model. The computation of the atmospheric loading effects follows Boy *et al.* (2002), that is, the atmospheric thickness is not neglected, but the air density variations with height are supposed to be only function of the surface pressure (Merriam 1992). The ocean loading effects are modelled as a thin-layer process.

The global pressure field are replaced by the local pressure measurements collocated with the gravimeter for a local cell with a radius 0.1° around the gravimeters. The ECMWF Reanalysis ERA-40 project (Uppala *et al.* 2005) ended in 2002 August, unlike the NCEP Reanalysis (Kalnay *et al.* 1996) with data available up to now almost in real time, therefore we had to combine data sets from different operational models. We also take the advantage of the 4-D variational assimilation operational implementation at the ECMWF (Rabier *et al.* 2000), starting in 1997 December to use surface pressure field data with a temporal resolution of 3 hr.

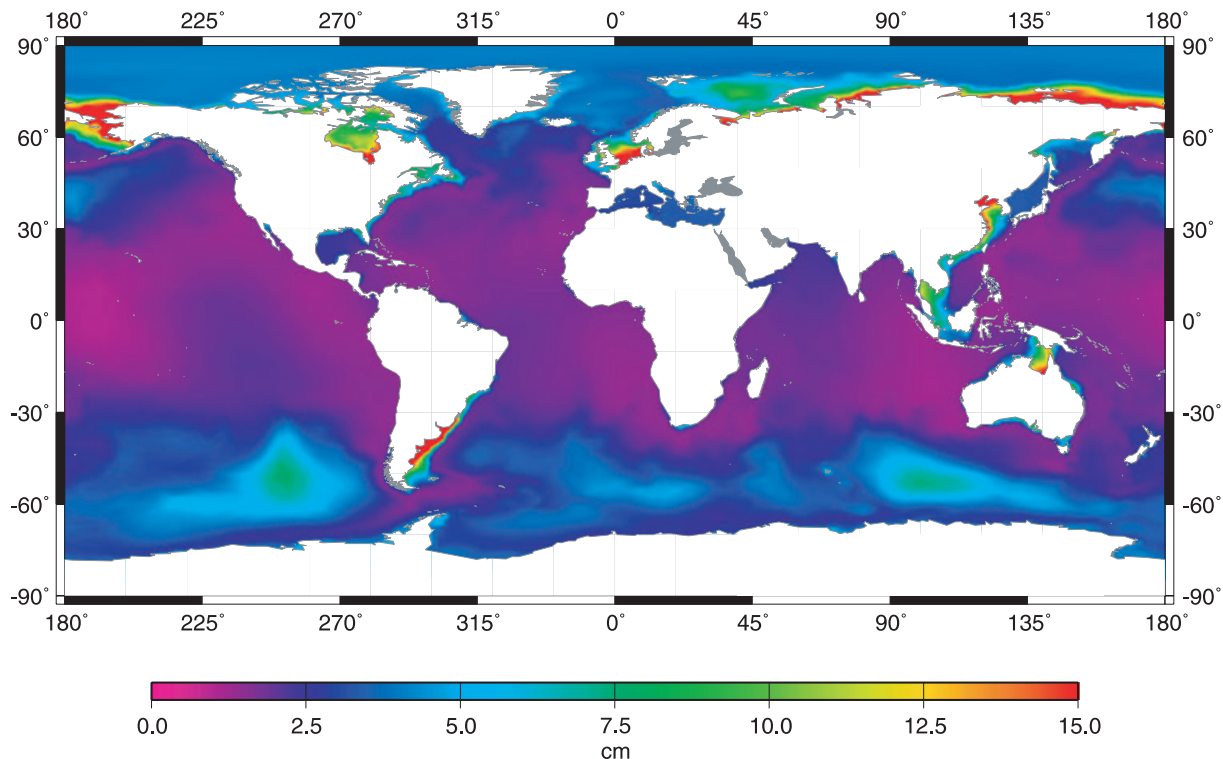


Figure 1. The rms differences (in cm) between the inverted barometer assumption and HUGO-m, computed for the 1997–2006 period.

For the ocean loading effects, sea height variations are depending on the choice of the ocean response to pressure forcing:

- (i) $h(\theta, \lambda, t) = 0$, for a non-inverted ocean response to pressure forcing.
- (ii) $h(\theta, \lambda, t) = -\frac{p(\theta, \lambda, t) - \bar{p}(t)}{\rho_w g_0}$ (where $\bar{p}(t)$ is the mean air pressure over the oceans), for an IB hypothesis.
- (iii) $h(\theta, \lambda, t)$ is the output of the barotropic models forced by pressure and winds, if the dynamic ocean response to pressure is taken into account.

3 REDUCTION OF SURFACE GRAVITY RESIDUALS

3.1 Processing of gravity data

We extract from the GGP global network (Crossley *et al.* 1999), 15 superconducting gravimeters (see Fig. 2 for their location). Raw

1-min gravity and pressure are classically pre-processed following Crossley *et al.* (1993), and then decimated to hourly samples.

Gravity are then corrected from polar motion and length-of-day induced effects (Wahr 1985), using EOPC04 series from the International Earth Rotation Service (IERS), assuming an elastic Earth and an equilibrium pole tide, including self-attraction and loading terms (Agnew & Farrell 1978). Long period tides (solid Earth and ocean tidal loading) are removed using Dehant *et al.* (1999) theoretical gravimetric factors and NAO99b ocean tide model (Matsumoto *et al.* 2000). The different atmospheric and oceanic loading corrections, that is, local pressure correction (barometric admittance), ECMWF-NIB, ECMWF-IB and ECMWF and HUGO-m, are then applied, before performing a tidal analysis using the ETERNA package (Wenzel 1997) in order to remove daily and subdaily solid Earth tide and ocean tidal loading contributions.

We choose not to correct for continental hydrology loading effects, as we have only access to global soil moisture and snow

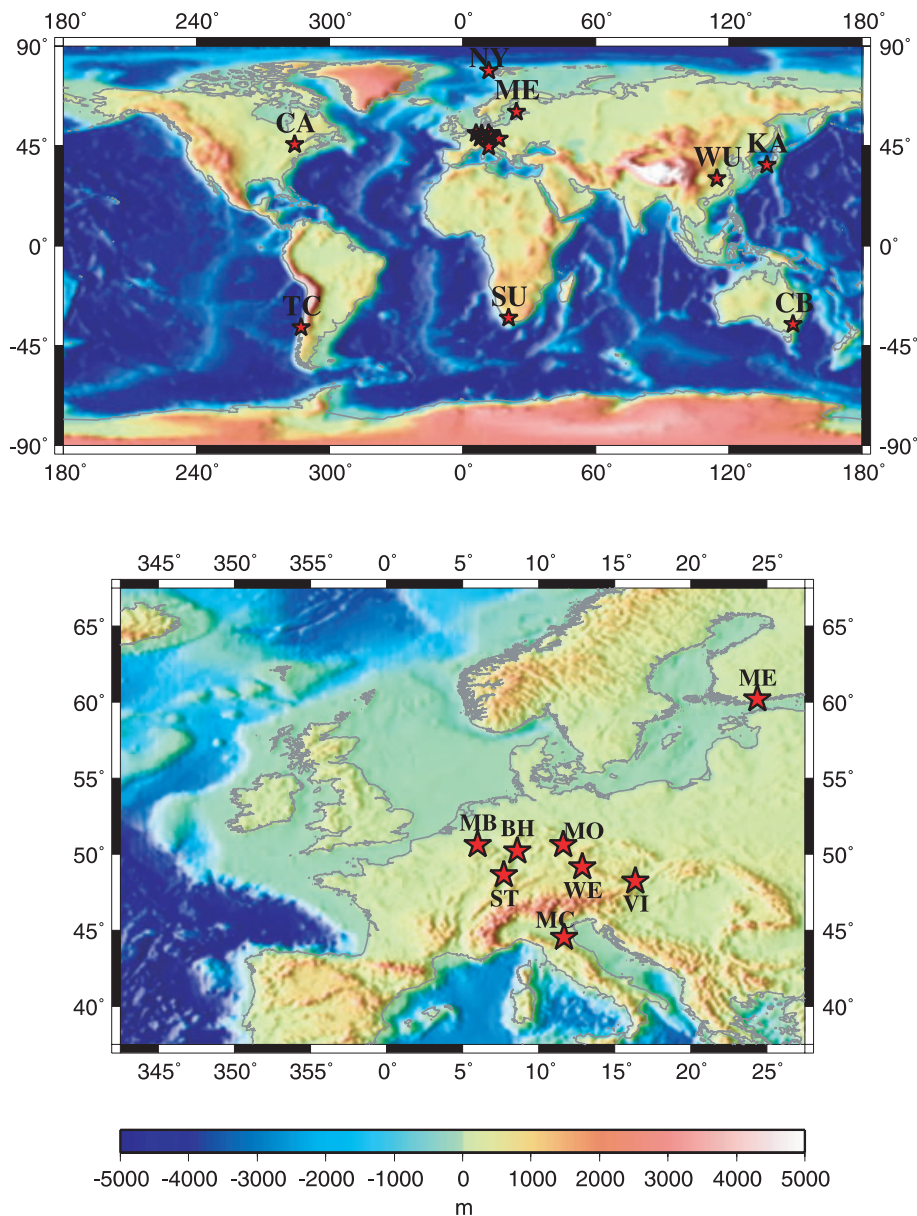


Figure 2. Location of the different superconducting gravimeters of the Global Geodynamics Project (GGP) network.

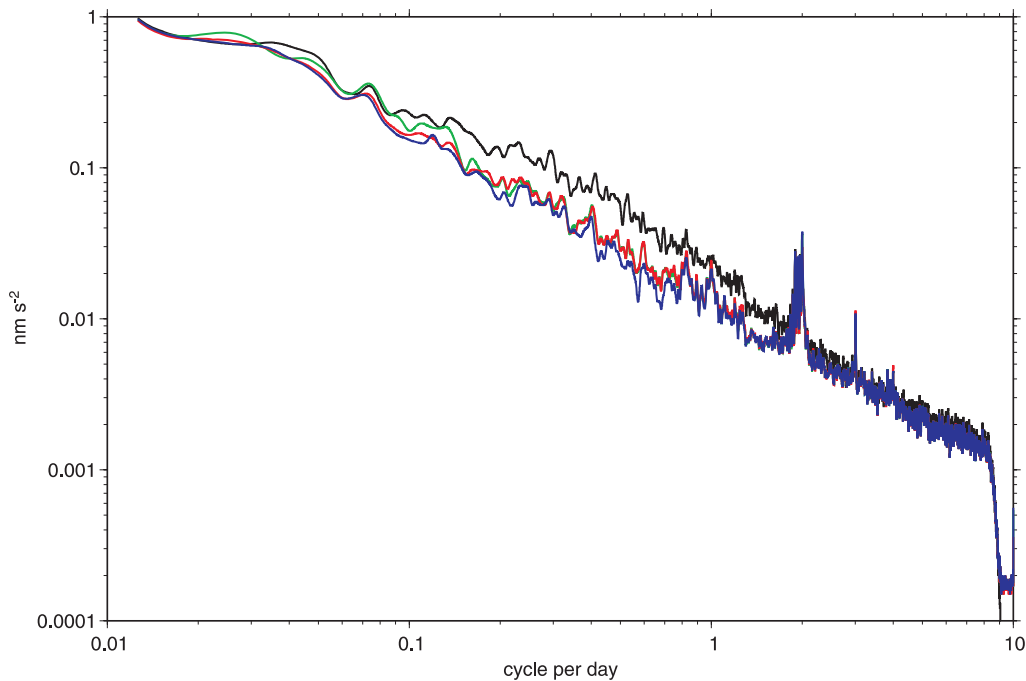


Figure 3. Spectrum of gravity residuals for the SG CO26 installed in Strasbourg, with the different atmospheric and oceanic loading correction, that is, local pressure correction (black), ECMWF-NIB (green), ECMWF-IB (red) and ECMWF+HUGO-m (blue).

models, such as Global Land Data Assimilation System (GLDAS) (Rodell *et al.* 2004). Due to their spatial sampling, they are not always able to recover all the short wavelength features near the gravimeters (Boy & Hinderer 2006). In order to improve hydrological loading computations, local measurements would be required (Van Camp *et al.* 2006), but they are not currently available for all instruments.

3.2 Results from tidal analyses

We compare the gravity residuals with the different atmospheric and oceanic corrections, and for the 15 superconducting gravimeters. Fig. 3 shows the spectrum of gravity residuals for the CO26 gravimeter, installed in Strasbourg (France), computed for the 1997–2007 period. We retrieve a similar result as Boy *et al.* (2002) using ECMWF rather than NCEP Reanalysis (Kalnay *et al.* 1996) surface pressure field, that is, that the IB hypothesis allows a reduction of gravity residuals compared to the local pressure correction and the NIB assumption, for periods up to a few months. However the differences between the global pressure correction using the ECMWF fields and the local pressure corrections are larger than using the NCEP Reanalysis fields, because of their higher spatial (up to approximately 0.25° in 2006) and temporal (3 hr after 1997 December) sampling (2.5° and 6 hr for NCEP Reanalysis). Some tidal signals in the diurnal and semi-diurnal bands are still left in the residuals, as well as a peak at S3 (8 hr) period.

The use of the barotropic HUGO-m ocean model, forced by ECMWF pressure and winds, allows a reduction of the gravity residuals for the Strasbourg instrument, for periods between typically one day and a few months. The improvement in term of reduction of residuals comes mainly from the modelling of the ocean variability over the North Sea and the Northwestern European shelf, as the

departure from the IB assumption are larger over shallow water regions (see Fig. 1).

As Boy *et al.* (2002) results are confirmed, we choose to plot on Fig. 4, gravity residuals with the ECMWF – IB and ECMWF + HUGO-m loading corrections for all superconducting gravimeters. Except for Kamioka (Japan) and Metsähovi (Finland) instruments, the residuals are lower with HUGO-m, compared to the IB assumption, for period between typically 1 d and 20–50 d. This is particularly true for Ny-Alesund (Svalbard), Sutherland (South Africa) and Canberra (Australia) which are close to coasts, and at high latitudes, that is, where the differences between the IB and HUGO-m are larger (see Fig. 1). Kamioka is the newest station (installed in 2004), but is an old version of superconducting gravimeter, such as the instrument installed in Metsähovi. For this gravimeter, the lack of the Baltic Sea in HUGO-m might be the reason of similar residuals with the two atmospheric and oceanic loading corrections.

Table 1 shows the mean amplitude of gravity residuals with the ECMWF-IB and ECMWF+HUGO-m loading corrections, for six different frequency bands: periods, respectively, larger than 1000 days, between 1000 and 250 days, between 50 and 250 days, between 10 and 50 days, 2 and 10 days and finally between 6 hr and 2 days. As shown on Fig. 4, non-tidal ocean loading corrections using HUGO-m, allow a systematic and significant reduction (10 per cent and more) of gravity residuals for period between a few days and about 50 days, compared to the IB assumption. For long (larger than 250 days) and short (smaller than 2 d) periods, there is no improvement in terms of reduction of the variance of gravity residuals.

4 EXAMPLES OF STORM SURGES IN EUROPE

Over continental shelves, air pressure and winds can cause large sea surface height variations, known as *storm surges*. Their amplitude

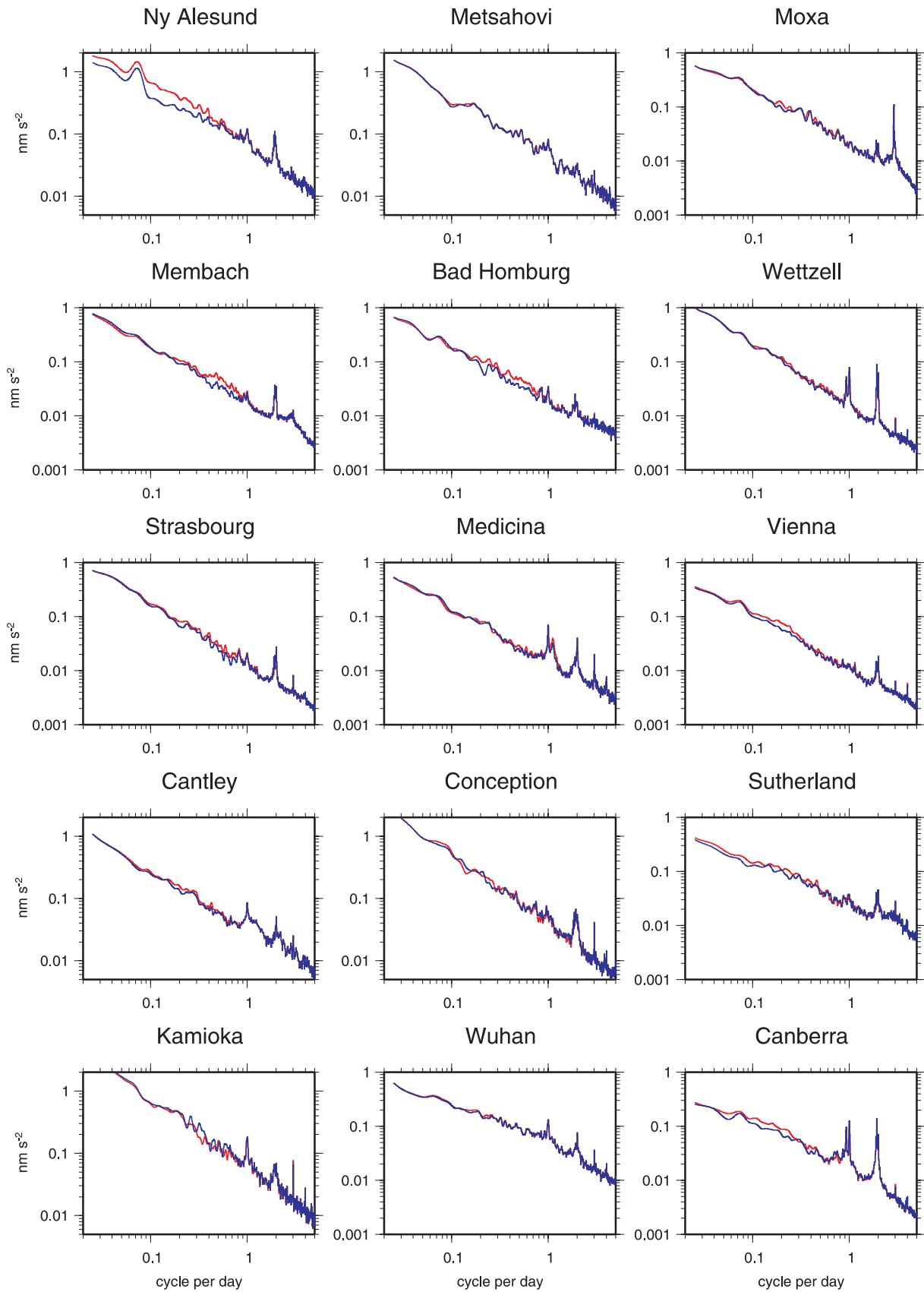
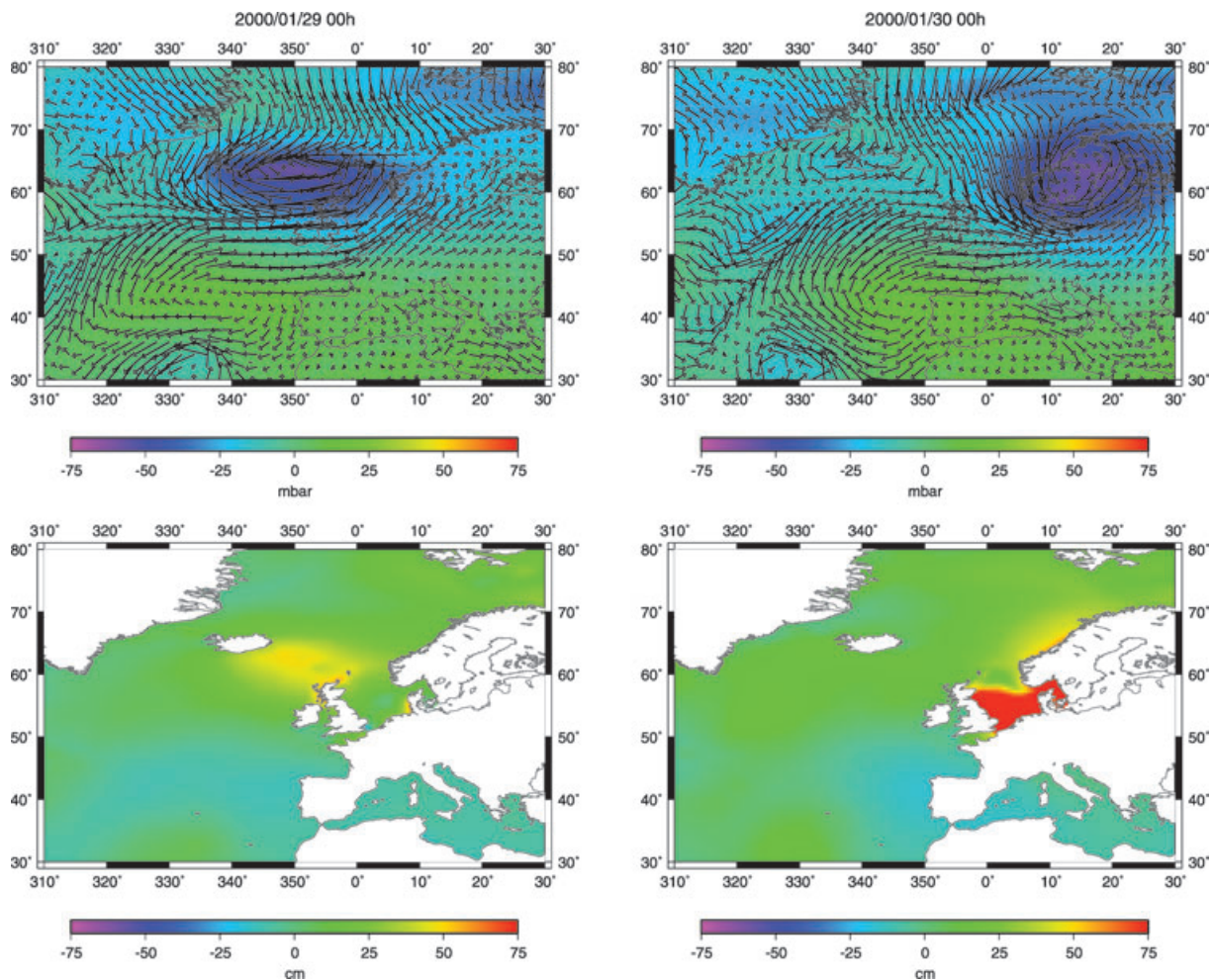


Figure 4. Spectrum of gravity residuals for all superconducting gravimeters, with the ECMWF-IB (red) and ECMWF+HUGO-m (blue) loading corrections.

Downloaded from https://academic.oup.com/gji/article/175/1/35/719316 by guest on 18 June 2021

Table 1. Amplitude of gravity residuals using ECMWF-IB and ECMWF+HUGO-m loading corrections, as a function of the period band.

| | $T > 1000$ d | | $250 < T < 1000$ d | | $50 < T < 250$ d | | $10 \text{ d} < T < 50$ d | | $2 \text{ d} < T < 10$ d | | $0.5 \text{ d} < T < 2 \text{ d}$ | |
|----|--------------|--------|--------------------|--------|------------------|--------|---------------------------|--------|--------------------------|--------|-----------------------------------|--------|
| | IB | HUGO-m | IB | HUGO-m | IB | HUGO-m | IB | HUGO-m | IB | HUGO-m | IB | HUGO-m |
| BH | 7.252 | 7.300 | 8.743 | 8.737 | 1.115 | 1.078 | 0.337 | 0.353 | 0.087 | 0.072 | 0.020 | 0.018 |
| CA | 10.096 | 10.040 | 10.121 | 10.152 | 2.181 | 2.176 | 0.500 | 0.487 | 0.121 | 0.110 | 0.036 | 0.036 |
| CB | 3.496 | 3.450 | 1.636 | 1.640 | 0.451 | 0.433 | 0.186 | 0.167 | 0.067 | 0.056 | 0.025 | 0.026 |
| KA | 39.138 | 39.141 | 47.693 | 47.658 | 11.347 | 11.405 | 1.530 | 1.524 | 0.274 | 0.299 | 0.063 | 0.067 |
| MB | 6.740 | 6.612 | 5.407 | 5.493 | 1.325 | 1.320 | 0.363 | 0.389 | 0.083 | 0.073 | 0.020 | 0.017 |
| MC | 3.244 | 3.268 | 7.128 | 6.958 | 0.964 | 0.914 | 0.269 | 0.277 | 0.057 | 0.057 | 0.018 | 0.017 |
| ME | 21.556 | 21.552 | 10.214 | 10.123 | 2.864 | 2.841 | 0.718 | 0.706 | 0.169 | 0.167 | 0.044 | 0.044 |
| MO | 5.264 | 5.339 | 3.912 | 4.039 | 1.105 | 1.090 | 0.345 | 0.356 | 0.093 | 0.087 | 0.020 | 0.020 |
| NY | 8.063 | 8.106 | 14.737 | 14.691 | 3.039 | 2.884 | 1.205 | 0.891 | 0.309 | 0.211 | 0.071 | 0.068 |
| ST | 22.316 | 22.401 | 6.764 | 6.808 | 0.970 | 0.983 | 0.385 | 0.375 | 0.069 | 0.061 | 0.013 | 0.012 |
| SU | 3.695 | 3.611 | 2.635 | 2.866 | 0.652 | 0.679 | 0.244 | 0.210 | 0.089 | 0.078 | 0.024 | 0.024 |
| TC | 19.683 | 19.728 | 64.303 | 64.711 | 7.141 | 7.158 | 1.084 | 1.048 | 0.187 | 0.186 | 0.041 | 0.044 |
| VI | 4.074 | 4.053 | 2.317 | 2.259 | 0.589 | 0.579 | 0.209 | 0.197 | 0.052 | 0.044 | 0.010 | 0.010 |
| WE | 35.947 | 35.851 | 19.150 | 19.143 | 1.689 | 1.678 | 0.463 | 0.469 | 0.081 | 0.077 | 0.019 | 0.018 |
| WU | 5.702 | 5.712 | 5.941 | 5.673 | 1.316 | 1.318 | 0.363 | 0.356 | 0.142 | 0.137 | 0.052 | 0.052 |

**Figure 5.** Surface pressure, winds (ECMWF) and sea surface height (HUGO-m) for the 2000 January 29 and 30, corresponding to the storm surge studied by Fratepietro *et al.* (2006).

can reach several metres in the North Sea. Fratepietro *et al.* (2006) compared gravity residuals at the Membach station to the loading computed with the Proudman Oceanographic Laboratory storm surge model, for an event in 2000 January–February (see Fig. 5).

We are extending this previous study to another storm surge which occurred in 2003 December, and to all available superconducting gravimeters installed in western Europe, and not only to the Membach instrument as it was done by Fratepietro *et al.* (2006).

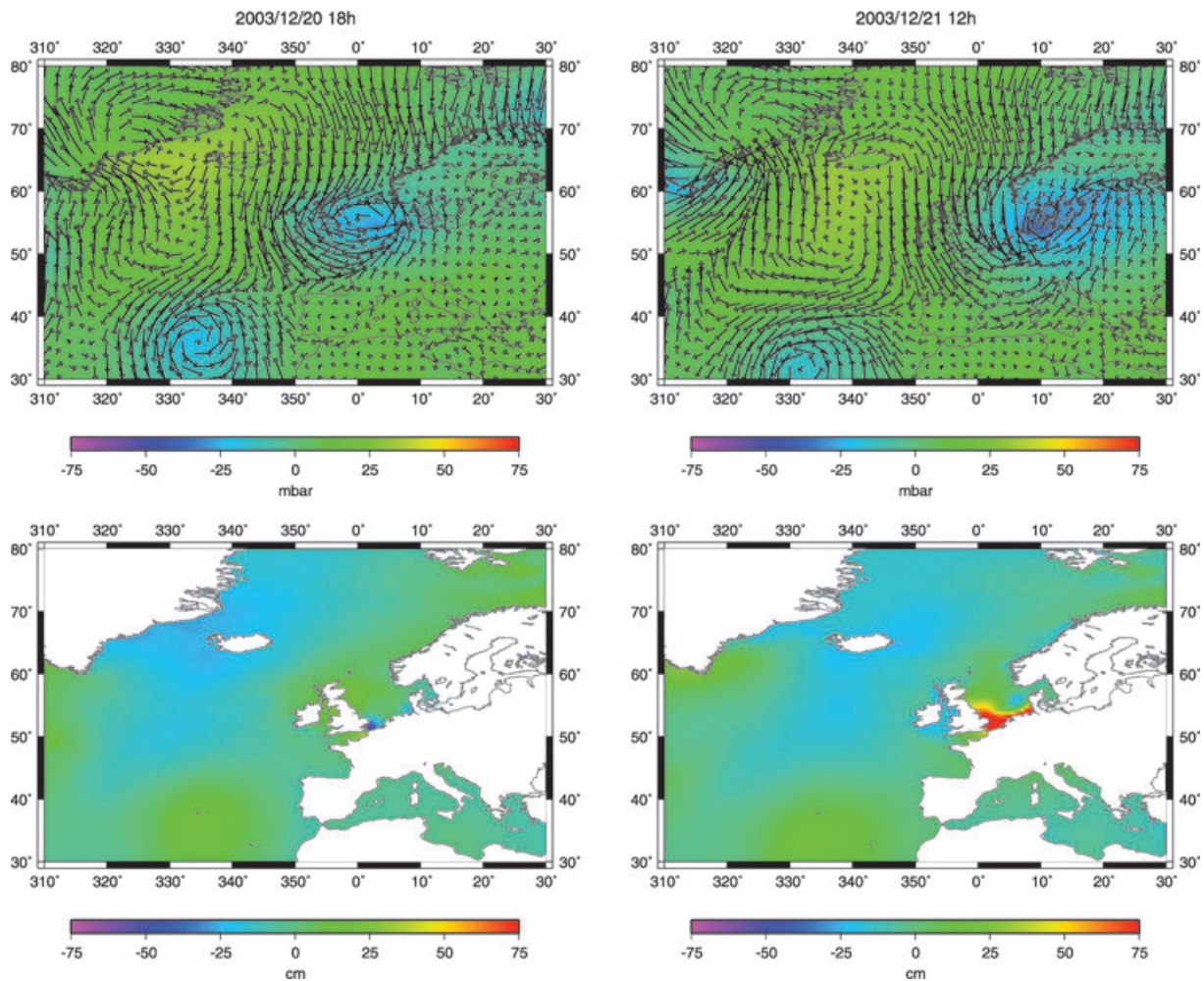


Figure 6. Same as Fig. 5, but for the 2003 December 20 and 21.

Despite its different temporal (6-hourly instead of hourly samples) and spatial resolution (0.5° instead of 12 km), we are still using the HUGO-m ocean model, instead of the POL barotropic model. However, the spatial resolution of the finite element grid of HUGO-m is about 20 km along the European coasts. Before comparing loading estimates to gravity residuals, we are first showing the agreement between HUGO-m sea surface height variations with several tide gauges along the North Sea coasts.

4.1 Comparison of HUGO-m sea height variations with tide gauges

Fig. 5 shows the surface pressure and wind variations from ECMWF, and the sea surface height variations from HUGO-m, for the 2000 January 29 and 30, showing the storm surge in the North Sea studied by Fratepietro *et al.* (2006). Due to the wind forcing, the amplitude of the sea surface height variations reached about 1 m, on the Belgian coasts the 30th of January.

The 2003 December storm surge is also shown in Fig. 6. Although the maximum amplitude is also larger than 1 m along the North Sea coasts, the spatial extend is much smaller compared to the 2000 event.

We extracted from various networks eight different tide gauge records, along the North Sea coasts. Figs 7 and 8 the good agree-

ment between HUGO-m sea surface height and detided tide gauge measurements for the 2000 and, respectively, 2003 storm surges. Despite the spatial (0.5°) and temporal (6 hr) sampling, HUGO-m barotropic ocean model is able to simulate the small wavelength features of the two surges. It allows us therefore to use HUGO-m model to estimate gravity loading effects, and not only dedicated storm surge models, such as the POL model used by Fratepietro *et al.* (2006).

4.2 Gravity variations

Fig. 9 shows the gravity residuals (corrected for tides, atmospheric loading and polar motion) for five different superconducting gravimeters in Europe, as well as the non-tidal ocean loading modelled with HUGO-m. For the Membach stations, we also plot the loading effects using the POL model (Fratepietro *et al.* 2006). In green is also shown the global hydrology loading effects (Boy & Hinderer 2006), estimated from soil-moisture and snow from the ECMWF Reanalysis (ERA40) project (Uppala *et al.* 2005). For Membach station, the agreement between gravity observations and loading estimates is better than Fratepietro *et al.* (2006), because of the different estimation of atmospheric loading effects. We compute the atmospheric loading using 3-hourly global surface pressure field provided by the ECMWF, whereas Fratepietro *et al.* (2006)

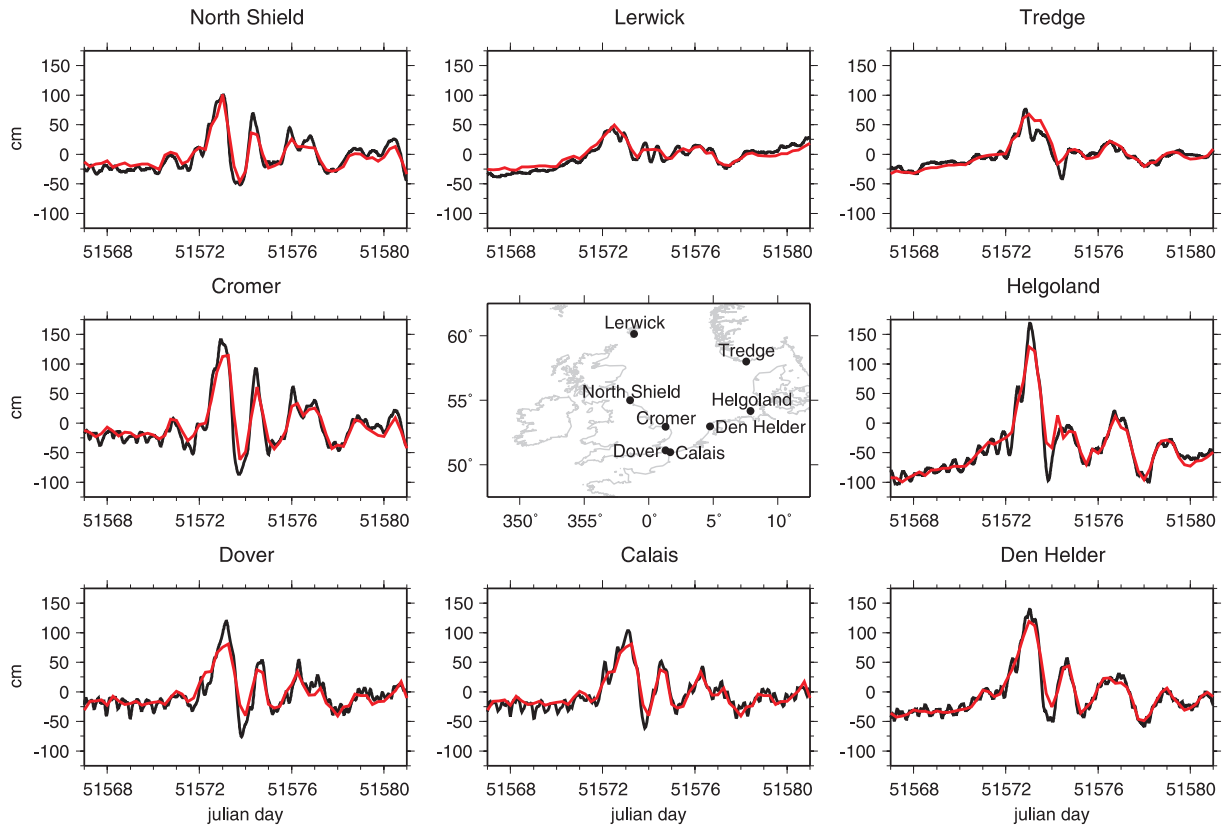


Figure 7. Comparison of HUGO-m sea surface height variations (red) with several tide gauges (black) along the North Sea coasts, for 2000 January and February.

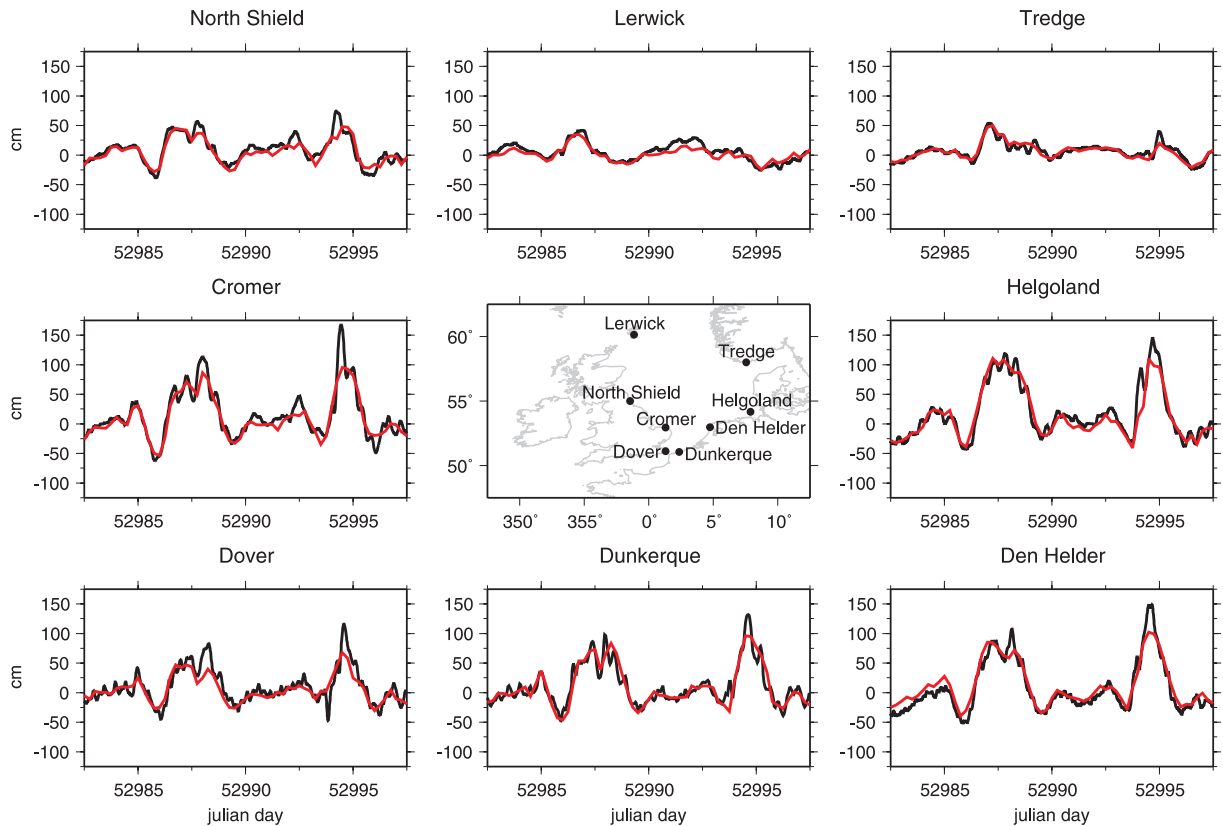


Figure 8. Same as Fig. 7, but for 2003 December.

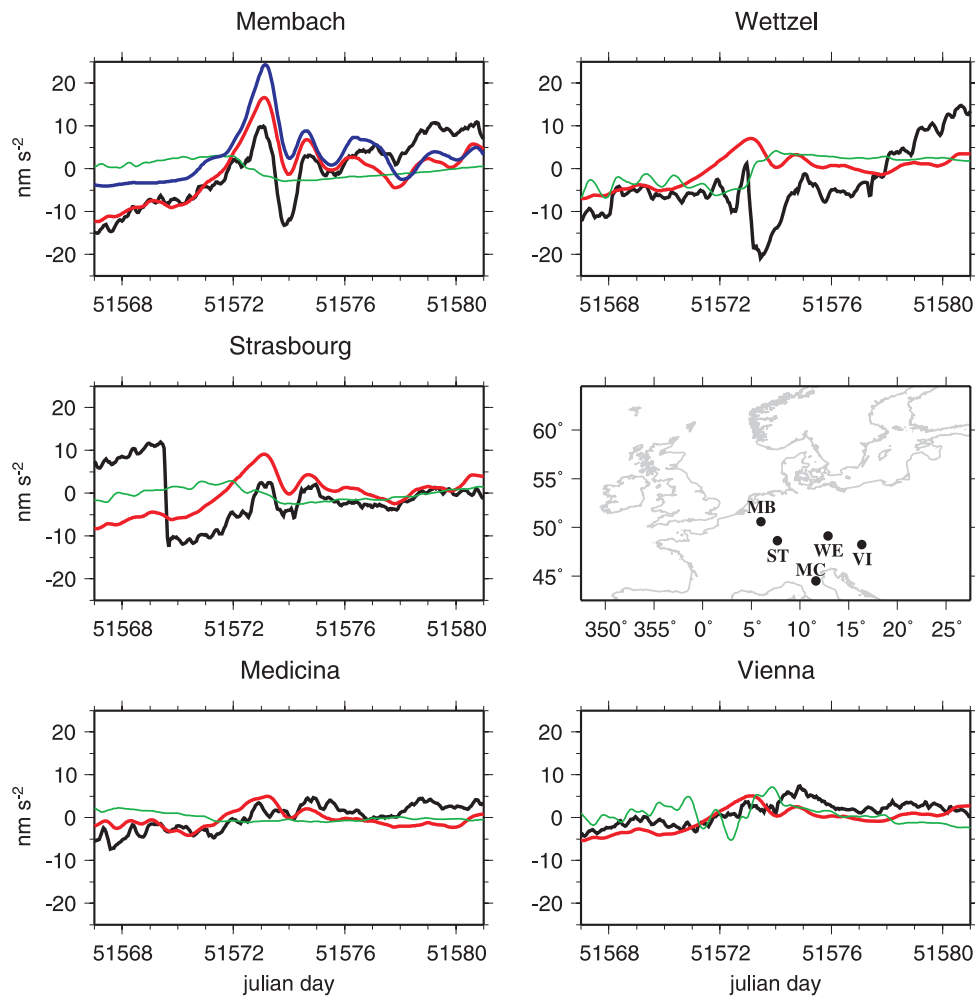


Figure 9. Gravity residuals (black) for various superconducting gravimeters in Europe and non-tidal ocean loading from HUGO-m model (red), the POL storm surge model (blue) and global hydrology (ECMWF Reanalysis) loading (green) for 2000 January and February.

removed atmospheric effects using only local air pressure and a linear admittance factor (Warburton & Goodkind 1977).

The non-tidal ocean loading amplitude decreases with the distance to the North Sea coasts, but still reaches about 10 nm s^{-2} ($1 \mu\text{gal}$) in Vienna. The large offset for Strasbourg the 2000 January 26 (Julian day equal to 51569) may be due by instrument noise, but not by a geophysical induced signal. Storms are often linked with heavy rainfall, but the ERA-40 soil-moisture model does not show large hydrological induced loading. However, the coarse resolution of the model (1.125°) may not be adequate to represent small wavelength and rapid rainfall events, and therefore, soil moisture changes. This is one of the reasons to extend this study to the 2003 December storm surge, in addition to the larger number of gravimeters at this time.

Fig. 10 shows the gravity residuals for eight instruments, the non-tidal ocean loading and the global hydrology loading using the state-of-the-art GLDAS (Rodell *et al.* 2004) hydrology model. Its spatial (0.25°) and temporal (3 hr) resolutions should be more adequate to estimate the soil-moisture changes associated with the storm. For Membach, Bad-Homburg, Strasbourg and Wettzell, it is clear that HUGO-m and GLDAS can explain the gravity variations for these two weeks. For the Metsähovi station, the large gravity variations cannot be explained, but HUGO-m does not include the Baltic Sea.

As shown by Virtanen & Mäkinen (2003) and Virtanen (2004), there is indeed a strong correlation between Metsähovi gravity residuals and tide gauge measurements in the Baltic sea. New versions of HUGO-m model now include the semi-enclosed basins, such as the Baltic and the Black Seas.

Table 2 gives the correlation coefficients between gravity residuals, non-tidal ocean loading, and hydrology loading for the two storm surges. For the 2000 January–February event, the correlation between gravity residuals and the ocean loading is higher than 0.5. The negative correlation for Strasbourg is due to the negative jump at the beginning of the time-series. Hydrological contribution estimated with ECMWF Reanalysis soil-moisture and snow models is correlated with gravity residuals only for Wettzell station.

As the 2003 December storm surge is smaller in amplitude than the 2000 January–February surge, the correlation between gravity residuals and HUGO-m estimated loading is also smaller. The correlation is larger than 0.5 only for Membach, Strasbourg and Vienna instruments. Another interesting result is the higher correlation between gravity and hydrology loading, estimated with GLDAS.

An improvement of the hydrology loading estimates would require, in addition to the global fields, local measurements of soil water content, as shown by Van Camp *et al.* (2006), but this is not the aim of the paper. However the differences between the two

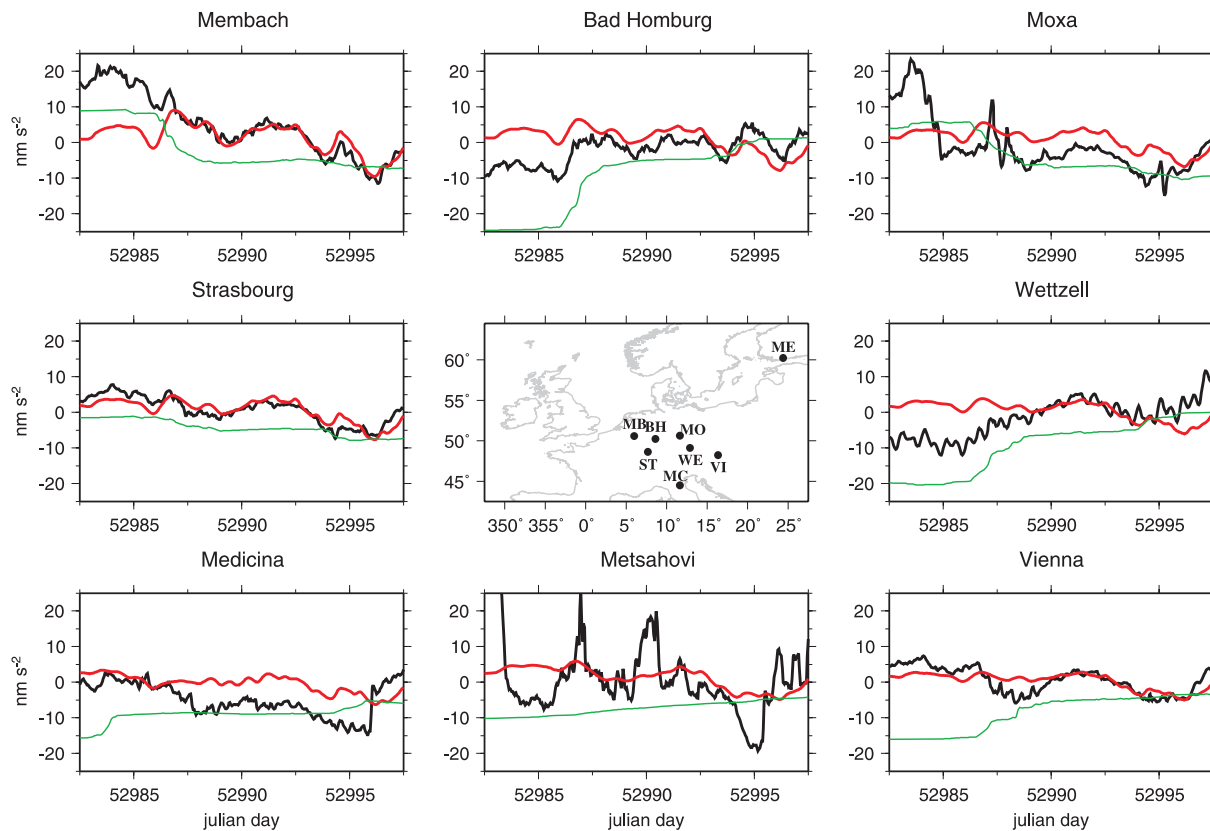


Figure 10. Same as Fig. 9, but for 2003 December, and GLDAS hydrology model (green).

Table 2. Correlation coefficients between gravity residuals, non-tidal ocean loading and hydrology loading, for the 2000 January–February and 2003 December storm surges.

| | 2000 January–February | | | 2003 December | | |
|----|-----------------------|--------------------|------------------|---------------------|--------------------|------------------|
| | Residual and HUGO-m | Residual and ERA40 | HUGO-m and ERA40 | Residual and HUGO-m | Residual and GLDAS | HUGO-m and GLDAS |
| BH | | | | 0.36 | 0.70 | −0.23 |
| MB | 0.83 | −0.42 | −0.52 | 0.55 | 0.77 | 0.20 |
| MC | 0.52 | −0.34 | −0.22 | 0.48 | 0.49 | −0.02 |
| ME | 0.71 | 0.73 | 0.86 | 0.25 | −0.53 | −0.39 |
| MO | | | | 0.34 | 0.46 | 0.21 |
| ST | −0.33 | −0.16 | −0.04 | 0.82 | 0.19 | 0.13 |
| VI | 0.81 | −0.19 | −0.19 | 0.69 | −0.52 | −0.32 |
| WE | 0.59 | 0.61 | 0.65 | 0.13 | 0.67 | −0.31 |

approaches would not change the agreement between gravity residuals and the non-tidal ocean loading effects, estimated with HUGO-m, for the 2003 December storm surge. However, ERA-40 resolution may not be sufficient to model the rapid and small wavelength soil moisture variations for 2000 January–February.

5 DISCUSSION AND CONCLUSION

We have shown that HUGO-m (Carrère & Lyard 2003) barotropic ocean model allows a systematic reduction of gravity residuals for all superconducting gravimeters, compared to the IB assumption, as previous used by Boy *et al.* (2002) in their atmospheric loading estimates. As the dynamic ocean response to pressure forcing does not differ from the static IB model at low frequencies, there is no decrease of gravity residuals for periods exceeding typically 50–100 d. On the other hand, although the departure from the IB

increases with the frequency, there is no evidence of reduction of gravity residuals for periods lower than a few days. Periods below typically 1 d should be improved using 3-hourly ECMWF pressure and winds, instead of 6-hourly samples, when forcing HUGO-m barotropic ocean model.

At seasonal timescales, the atmospheric and non-tidal oceanic loading effects are not anymore the main source of gravity variations. They are mainly due to continental hydrology (Boy & Hinderer 2006), which can be modelled using global hydrology models (soil moisture and snow) such as GLDAS (Rodell *et al.* 2004), and also local measurements (Van Camp *et al.* 2006).

Because of their sensitivity, and their vicinity to the coasts (usually distances less than 1000 km), superconducting gravimeter processing requires a model with a high spatial sampling rate, such as HUGO-m. Models like PPHA (Flechtner 2005) with resolution larger than 100 km cannot be used to correct gravity observations

from non-tidal oceanic loading, as they are not able to represent correctly sea height variations over shallow water regions, although the differences between these models are quite small on open oceans.

However, HUGO-m ocean model allows a precise estimation of short period non-tidal ocean loading over the North Sea, in the case of large storm surges. The comparison with the previous study by Fratepietro *et al.* (2006) shows the importance of a precise atmospheric correction, using global pressure field instead of the local pressure alone, for an accurate estimation of gravity residuals, even at high frequencies. As storms are associated with rapid variations of the vertical profile of temperature, an improvement of the atmospheric loading estimates will require to compute the complete 3-D atmospheric correction (Neumeyer *et al.* 2004), as it is done operationally for space gravity mission processing (Boy & Chao 2005).

ACKNOWLEDGMENTS

We thank all the GGP members for providing high quality minute gravity and pressure data. We also thank European Sea Level Service (ESEAS) (<http://www.e seas.org/>), British Oceanographic Data Center (BODC) (<http://www.bodc.ac.uk/>) and Système d'Observation du Niveau des Eaux Littorales (SONEL) (<http://www.sonel.org/>) for providing the tide gauge measurements.

REFERENCES

- Agnew, D.C. & Farrell, W.E., 1978. Self-consistent equilibrium ocean tides, *Geophys. J. R. astr. Soc.*, **55**, 171–181.
- Boy, J.-P. & Chao, B.F., 2005. Precise evaluation of atmospheric loading effects on Earth's time-variable gravity field, *J. geophys. Res.*, **110**, B08412, doi:10.1029/2002JB002333.
- Boy, J.-P. & Hinderer, J., 2006. Study of the seasonal gravity signal in superconducting gravimeter data, *J. Geodyn.*, **41**, 227–233.
- Boy, J.-P., Gegout, P. & Hinderer, J., 2002. Reduction of surface gravity data from global atmospheric pressure loading, *Geophys. J. Int.*, **149**, 534–545.
- Carrère, C. & Lyard, F., 2003. Modeling the barotropic response of the global ocean to atmospheric wind and pressure forcing—comparisons with observations, *Geophys. Res. Lett.*, **30**(6), 1275, doi:10.1029/2002GL016473.
- Crossley, D.J., Hinderer, J., Jensen, O. & Xu, H., 1993. A slewrates detection criterion applied to SG data processing, *Bull. d' Inf. Marées Terr.*, **117**, 8675–8704.
- Crossley, D.J. *et al.*, 1999. Network of superconducting gravimeters benefits several disciplines, *EOS, Trans. Am. geophys. Un.*, **80**, 121–126.
- Dehant, V., Defraigne, P. & Wahr, J., 1999. Tides for a convective Earth, *J. geophys. Res.*, **104**(B1), 1035–1058.
- Dobslaw, H. & Thomas, M., 2005. Atmospheric induced oceanic tides from ECMWF forecasts, *Geophys. Res. Lett.*, **32**, L10615, doi:10.1029/2005GL022990.

- Farrell, W.E., 1972. Deformation of the Earth by surface loads, *Rev. Geophys. Space Phys.*, **10**, 761–797.
- Flechtner, F., 2005. GRACE AOD1B Product Description Document, *JPL-327-750* (GR-GFZ-AOD-0001), Rev. 2.1.
- Fratepietro, F., Baker, T.F., Williams, S.D.P. & Van Camp, M., 2006. Ocean loading deformations caused by storm surges on the northwest European shelf, *Geophys. Res. Lett.*, **33**, L06317, doi:10.1029/2005GL025475.
- Hirose, N., Fukumori, I., Zlotnicki, V. & Ponte, R.M., 2001. Modeling the high-frequency barotropic response of the ocean to atmospheric disturbances: sensitivity to forcing, topography and friction, *J. geophys. Res.*, **106**(C12), 30 987–30 995.
- Kalnay, E. *et al.*, 1996. The NCEP/NCAR 40-year reanalysis project, *Bull. Amer. Meteor. Soc.*, **77**, 437–470.
- Lemoine, J.-M., Bruinsma, S., Loyer, S., Biancale, S., Marty, J.-C., Perosanz, F. & Balmino, G., 2007. Temporal gravity field models inferred from GRACE data, *Adv. Space Res.*, **39**, 1620–1629.
- Matsumoto, K., Takanezawa, T. & Ooe, M., 2000. Ocean Tide Models Developed by Assimilating TOPEX/POSEIDON Altimeter Data into Hydrodynamical Model: a Global Model and a Regional Model Around Japan, *J. Oceanogr.*, **56**, 567–581.
- Merriam, J.B., 1992. Atmospheric pressure and gravity, *Geophys. J. Int.*, **109**, 488–500.
- Neumeyer, J., Hagedoorn, J., Leitloff, J. & Schmidt, T., 2004. Gravity reduction with three-dimensional atmospheric pressure data for precise ground gravity measurements, *J. Geodyn.*, **38**(3–5), 437–450.
- Rabier, F., Järvinen, H., Klinker, E., Mahfouf, J.-F. & Simmons, A., 2000. The ECMWF operational implementation of four-dimensional variational assimilation. I: experimental results with simplified physics, *Q. J. R. Met. Soc.*, **126**, 1143–1170.
- Rodell, M. *et al.*, 2004. The Global Land data assimilation system, *Bull. Amer. Meteor. Soc.*, **85**(3), 381–394.
- Uppala, S.M. *et al.*, 2005. The ERA-40 re-analysis, *Q. J. R. Meteorol. Soc.*, **131**, 2961–3012.
- Van Camp, M., Vanclooster, M., Crommen, O., Petermans, T., Verbeeck, K., Meurers, B., van Dam, T. & Dassargues, A., 2006. Hydrogeological investigations at the Membach station, Belgium, and application to correct long periodic gravity variations, *J. geophys. Res.*, **111**, B10403, doi:10.1029/2006JB004405.
- Virtanen, H., 2004. Loading effects in Metsähovi from the atmosphere and the Baltic Sea, *J. Geodyn.*, **38**, 407–422.
- Virtanen, H. & Mäkinen, J., 2003. The effect of the Baltic Sea level on gravity at the Metsähovi station, *J. Geodyn.*, **35**, 553–565.
- Wahr, J.M., 1985. Deformation induced by polar motion, *J. geophys. Res.*, **90**(B11), 9363–9368.
- Warburton, R.J. & Goodkind, J.M., 1977. The influence of barometric pressure variations on gravity *Geophys. J. R. astr. Soc.*, **48**, 3, 281–292.
- Wenzel H.G., 1997. The nanogal software: Earth tide data processing package ETERNA 3.30, *Bull. d' Inf. Marées Terr.*, **124**, 9425–9439.
- Wunsch, C. & Stammer, D., 1997. Atmospheric loading and the oceanic inverted barometer effect, *Rev. Geophys.*, **35**, 79–107.
- Zerbini, S., Matonti, F., Raicich, F., Richter, B. & van Dam, T., 2004. Observing and assessing nontidal ocean loading using ocean, continuous GPS and gravity data in the Adriatic area, *Geophys. Res. Lett.*, **31**, L23609, doi:10.1029/2004GL021185.